Altruistic Coordination Strategy for On-Ramp Merging on Highway of a Formation of Cooperative Automated Vehicles

1st Lyes Saidi
Heudiasyc, UMR CNRS 7253
Université de Technologie de Compiègne
Compiègne, France
lyes.saidi@hds.utc.fr

2nd Lounis Adouane
Heudiasyc, UMR CNRS 7253
Université de Technologie de Compiègne
Compiègne, France
lounis.adouane@hds.utc.fr

3rd Reine Talj
Heudiasyc, UMR CNRS 7253
Université de Technologie de Compiègne
Compiègne, France
reine.talj@hds.utc.fr

***Abstract*—It is getting increasingly recognized that, to get full advantage from Automated Vehicles (AVs), a number of situations involving multiple AVs will compulsory require the coordination of their relative activities and movements. Under the Multi-Vehicle Systems (MVS) paradigm, instead of considering individually each AV, it is proposed to create with several AVs a group that evolves under a certain coordination strategy. In this paper, it is proposed to utilize Cooperative Automated Vehicles (CAVs) synchronization ability to tackle one challenging scenario: on-ramp merging on highway. The main contribution of this paper is an overall collaborative approach, called Altruistic Formation Reconfiguration Strategy (AFRS), based on a multi-criteria optimization, to guarantee the safety and the energetic efficiency of CAVs, performing on-ramp merging on highway. Under the AFRS, it is proposed the extension of the Constrained Optimal Reconfiguration Matrix (CORM) [1] in order to overcome the CORM limitations, while guarantying both the CAV's non-collision requirement and the smooth collaborative navigation of the fleet. Several simulations are performed to evaluate the safety and reliability of the proposed approach.**

***Index Terms*—Cooperative Automated Vehicles, Altruistic Decision-Making, On-Ramp Merging on Highway.**

I. Introduction

The widespread of Intelligent Transportation Systems (ITS) is driven by the need to reduce accidents caused by human errors. Nevertheless, *individual* Automated Vehicles (AVs) are still insufficient, in view of the fact that a number of driving situation demand *coordination* among them. Cooperation between AVs at urban intersections, highway fleet navigation, and on-ramp merging on highway can not only prevent accidents but also reduce road congestion and improve energy efficiency [2]

In conflicting scenarios (e.g., intersection crossing, highway merging, etc.), MVS motion coordination and synchronization ability permits to establish collision avoidance strategies, what improves road safety. Cooperative Automated Vehicles (CAVs) can provide shorter gaps between vehicles and shorter responses time while improving the road capacity by identifying appropriate velocity [3]. According to [4], CAVs are capable of sensing more accurately, processing more information, and can be more tightly controlled, they benefit more from information offered by connectivity and road preview, which can lead to auspicious energy efficiency potentials.

In this paper, it is proposed to take advantage from the CAVs abilities to tackle one challenging scenario: on-ramp merging on highway. The difficulty of the considered scenario resides on the shared nature of the merging zone. In order to avoid collisions between the merging CAV and the CAVs present on the highway, the merging CAV has to discern whether to accelerate or decelerate to enter the highway. Meanwhile, the mainline users may have to modify their speeds to permit the entrance of the merging CAV, thus affecting traffic flow which may result in road congestion.

The main contribution of this paper is the Altruistic Formation Reconfiguration Strategy (AFRS). The first objective of the AFRS is to guarantee a safe and smooth reconfiguration of the MVS during the merging scenario. To this aim the Extended Constrained Reconfiguration matrix algorithm (E-CORM) was developed. The E-CORM uses the formal approach for formation modeling and reconfiguration developed in [1] [5] to coordinate the motion of the CAVs. A multi-mode decision-making strategy is the second objective of the AFRS. The decision-making level has the responsibility of switching between the nominal merging mode and the coordination mode.

The remainder of the paper is organized as follows. In Section II, the related work to the on-ramp merging scenario is discussed, in addition to the objectives of the AFRS. In Section III, we introduce the nomenclature used in the paper and the problem statement. The proposed AFRS is discussed in Section IV. The Section V presents the conducted simulations. We draw conclusions and set perspectives in Section VI.

II. Related work and objectives

Given the shared nature of the merging zone, one solution to the merging conflict is to synchronize the CAVs motions in order to avoid the presence of two or more vehicles in the shared zone at the same moment. In [3], the authors classified the on-ramp merging based literature into two categories, the centralized and the distributed approaches. (1) It relays on the

central controller to decide for all the vehicles (e.g., reservation approaches [6] [7], optimization-based approaches [8]). (2) Each vehicle defines its policy based on its information and the others broadcasted and/or shared data with the help of the Vehicle-to-Everything (V2X) communication (e.g., virtual mapping [9]).

Approaches based on the virtual platooning are also part of the literature. The concept of virtual platooning introduced in 1999 [10] is based on the virtual mapping onto the main road of the merging CAV's pose before the actual merging, allowing a safer and smoother merging behavior [11]).

Defining a safe passing sequence used by the CAVs to travel through the merging zone is one concept that can be used to tackle the merging scenario [12]. In [13], the authors proposed a grouping-based cooperative driving strategy for on-ramp merging on highway. The passing sequence was obtained through an optimization of the time spent in the merging area by each considered group. The approaches based on the definition of the passing sequence are often correlated with the presence of the V2X communication [14] [15].

Based on the communication range of the Road Side Unit (RSU) (cf. Figure 2), the CAVs present in the merging environment can be identified and attributed a personal ID. The details related to the communication level are out of the scope of this paper. The formation modeling used in this paper is inspired from the CORM formal formation modeling [1]. A reference CAV is defined; and based on its position, a mobile Frenet reference frame is created. As the CORM algorithm, the E-CORM algorithm takes advantage from the virtual structure approach to model and reconfigure the shape of the formation.

The CORM algorithm uses a restricted motion convergence approach which limits its flexibility. Thus, the main objective behind the proposed E-CORM algorithm, part of the AFRS, is to overcome the limitation encountered with the CORM in [1], while ensuring a safe and flexible formation reconfiguration.

The second objective of the AFRS resides in the proposed multi-mode decision-making. The decision level adopted in this paper has the responsibility of switching between: (1) the nominal mode, where the merging scenario is performed from the perspective of the merging CAV, when there is no conflict with other road occupants, and the non-collision requirement is ensured even without cooperation. (2) The coordination level is activated when the nominal mode fails to ensure the safety requirement. It is responsible of setting an optimal passing order given to the E-CORM algorithm to coordinate the motions of the CAVs in a safe and feasible manner.

III. Preliminaries and problem statement

This section is dedicated to the presentation of the main nomenclature used in this paper, along with the vehicle modeling and control law.

A. Preliminaries

In addition to this section where the used nomenclature in this paper is presented, please confer to Figures 2 and 6.

- $N \in \mathbb{N}$ is the number of the considered CAVs that are in the communication range, referred to individually by i, and $\mathcal{N} = \{1, ..., N\}$ is the set representing all the CAVs indices.
- The subset $\mathcal{M}$ with $\mathcal{M} \in \mathcal{N}$ contains only the m-indexes of the merging CAVs (CAV$_m$), $\mathcal{H}$ with $\mathcal{H} \in \mathcal{N}$ contains only the hw-indexes of the highway CAVs (CAV$_{hw}$). Consequently, $\mathcal{N} \equiv \mathcal{M} \bigcup \mathcal{H}$ and $\mathcal{M} \times \mathcal{H} = 0$.
- The pose in the global frame $\{X_G, Y_G\}$ of CAV$_i$ is defined by $X = [x, y, \theta]^T$ and its dynamic is referred to by $[\mathcal{V}, \delta]^T$ for linear velocity and steering angle, respectively.
- The coordinates of CAV$_i$ w.r.t. the mobile reference frame centered on CAV$_R$ are h_i and l_i for longitudinal and lateral coordinates respectively.
- $f_i = [h_i, l_i]^T$ is CAV$_i$ coordinates in the formation, $F = [f_1^T, ..., f_N^T]^T$ is the vector of coordinates of the formation composed of $N, N \in \mathcal{N}$ CAVs.
- T_{d_i} is the CAV$_i$ virtual target used by the virtual structure to control the shape of the formation. For the knowledge of the reader, further details can be found in [1].
- sq is the passing sequence of the CAVs in the merging zone.
- The collision time is known as CT, and CP is the collision partner.

B. Vehicle modeling and control law

The CAV is modeled using the tricycle model in [16]. A single front wheel replaces the two front wheels, and it is placed in-between them. The equations of the kinetic model can be written as:

$$\begin{aligned} \dot{x} &= \mathcal{V}\cos(\theta) \\ \dot{y} &= \mathcal{V}\sin(\theta) \\ \dot{\theta} &= \mathcal{V}/l_b \tan(\delta) \end{aligned} \tag{1}$$

with $X = [x, y, \theta]^T$, l_b, $\mathcal{V}$ and δ are the vehicle's pose, its wheelbase, linear velocity and steering angle respectively. The latter is expressed as $\delta = \arctan(l_b C_c)$ where $C_c = 1/R$, with R is the radius of the road and Cc its curvature.

To achieve the dynamic $[\mathcal{V}, \delta]$, the control law in this paper is based on the one developed in [17].

IV. Altruistic Formation Reconfiguration Strategy (AFRS)

As stated in Section II, the main objective of the Altruistic Formation Reconfiguration Strategy (AFRS) is to ensure the safety and the feasibility of the driving behavior of the CAVs during the merging scenario. To this aim, the AFRS (cf. Figure 1) is composed of two levels: (1) the multi-mode decision-making level (cf. Section IV-B), responsible of the activation of the proper behavior of the CAVs between the nominal mode (cf. Section IV-B1) and the cooperation mode (cf. Section IV-B2) depending on the safety of the supposed merging (cf. Figure 1, Behavior selection level). (2) The local trajectory planning level responsible of the generation of the dynamic targets T_d (cf. Figure 1, Local trajectory planning)

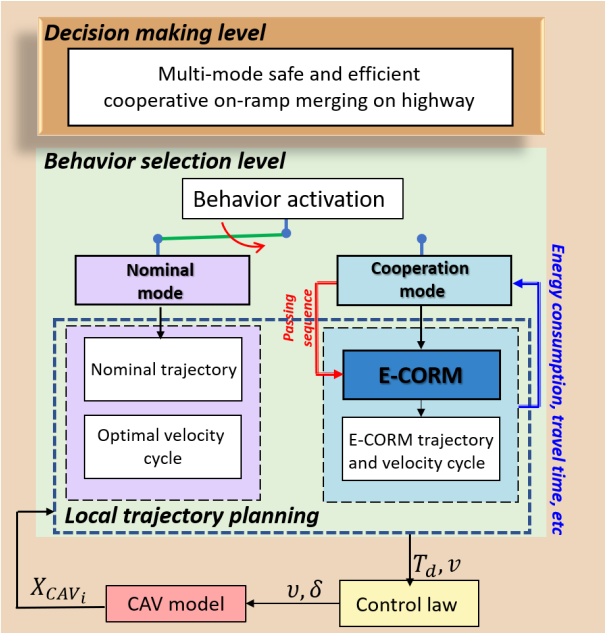

Fig. 1. Altruistic Formation Reconfiguration Strategy (AFRS)

and composed of the proposed E-CORM algorithm (cf. Section IV-A) that ensures the safety and flexibility of the formation reconfiguration, in addition to the nominal trajectory and velocity cycle generator attached to the nominal mode.

A. E-CORM: Extended Dynamic Reconfiguration Matrix

Before the presentation of the details of the proposed Extended Dynamic Reconfiguration Matrix (E-CORM) for formation reconfiguration. For the clarity of the paper and the understanding of the reader, the fundamentals about the formalization used to represent the formation are given. For further details on the adopted formation modeling formalism, the reader in invited to read [1].

For a formation composed of N CAVs, a reference CAV_R is defined to determine the coordinates of the CAVs part of the formation. The E-CORM uses a system of coordinates based on the Frenet reference frame w.r.t. CAV_R's pose, where h and l are the longitudinal and the lateral Frenet coordinates, respectively. These coordinates, transformed to the global reference frame permit to generate the pose of the virtual target T_d followed by the CAV. Further details about the used system of coordinates and virtual targets generation are given in [1].

The merging maneuver shown in Figure 2 consists of a formation reconfiguration. In other terms, the initial coordinates of the formation F^{init} are reshaped to match the desired coordinates F^{end}, corresponding to the formation coordinates at the end of the merging maneuver. $F(t)$ are the intermediate coordinates used to reshape the formation. Consequently, based on $F(t)$, the virtual dynamic targets $T_d(t)$ are generated for each CAV part of the formation.

$$\begin{cases} F^{init} = [f_1^{init^T}, ..., f_N^{init^T}]^T, \\ F^{end} = [f_1^{end^T}, ..., f_N^{end^T}]^T, \\ F(t) = [f_1(t)^T, ..., f_N(t)^T]^T, \end{cases} \tag{2}$$

$f_i^{init}, f_i^{end}, i \in \mathcal{N}$ are the coordinates of CAV$_i$ in the initial and final formation, while $f_i(t), i \in \mathcal{N}$ are its instantaneous coordinates.

The convergence error between the desired coordinates of CAV$_i$ in the formation and the actual ones is $e_{f_i} = [e_{h_i}, e_{l_i}]^T$, it can be defined as:

$$\begin{cases} e_{f_i} = f_i^{end} - f_i(t), \\ f_i(t) = [h_i(t), l_i(t)]^T, \\ f_i^{end} = [h_i^{end}, l_i^{end}]^T, \end{cases} \tag{3}$$

with $e = [e_{f_i}^T, ..., e_{f_N}^T]^T$ the convergence error vector.

In order to characterize the evolution of the reconfiguration from the initial shape toward the desired one, while ensuring the respect of the minimum inter-target distance d_{safety} between the N CAVs part of the formation, the E-CORM proposes an intermediate state vector S given in eq. (4).

$$S = \dot{e} + \lambda e + \gamma \int e \, dt \tag{4}$$

To overcome the CORM lack of flexibility, the E-CORM uses in addition to the convergence error e, the convergence rate $\dot{e}$ of the error and the sum of the errors through the integrative term of the latter. λ, $\gamma \in \mathbf{R}^+$ are the convergence gains and permit to offer more flexibility to the E-CORM algorithm.

The convergence of S follows a first order convergence model detailed in eq. (5).

$$\dot{S} = A \times S = A\dot{e} + A\lambda e + A\gamma \int e \, dt \tag{5}$$

where $A^{2N \times 2N}$ is a negative-definite convergence matrix.

Using eq. (3) in eq. (5) permits to write the extended system of equations representing the studied system.

$$\begin{aligned} \dot{S}_{h_1} &= a_{h_1}\dot{e}_{h_1} + a_{h_1}\lambda_{h_1}e_{h_1} + a_{h_1}\gamma_{h_1}\int e_{h_1}dt \\ \dot{S}_{l_1} &= a_{l_1}\dot{e}_{l_1} + a_{l_1}\lambda_{l_1}e_{l_1} + a_{l_1}\gamma_{l_1}\int e_{l_1}dt \\ &\vdots \\ \dot{S}_{h_N} &= a_{h_N}\dot{e}_{h_N} + a_{h_N}\lambda_{h_N}e_{h_N} + a_{h_N}\gamma_{h_N}\int e_{h_N}dt \\ \dot{S}_{l_N} &= a_{l_N}\dot{e}_{l_N} + a_{l_N}\lambda_{l_N}e_{l_N} + a_{l_N}\gamma_{l_N}\int e_{l_N}dt \end{aligned} \tag{6}$$

where h_i and l_i, representing the longitudinal and the lateral coordinates of the formation, converge toward the target with different convergence rates a_{h_i} and a_{l_i}.

The system in eq. (7) presents the matrix form of the studied system.

$$\begin{bmatrix} \dot{S}_{h_1} \\ \dot{S}_{l_1} \\ \dot{S}_{h_2} \\ \dot{S}_{l_2} \\ \vdots \\ \dot{S}_{h_N} \\ \dot{S}_{l_N} \end{bmatrix} = \Omega_1 \begin{bmatrix} \dot{e}_{h_1} \\ \dot{e}_{l_1} \\ \dot{e}_{h_2} \\ \dot{e}_{l_2} \\ \vdots \\ \dot{e}_{h_N} \\ \dot{e}_{l_N} \end{bmatrix} + \Omega_2 \begin{bmatrix} e_{h_1} \\ e_{l_1} \\ e_{h_2} \\ e_{l_2} \\ \vdots \\ e_{h_N} \\ e_{l_N} \end{bmatrix} + \Omega_3 \begin{bmatrix} \int e_{h_1} \, dt \\ \int e_{l_1} \, dt \\ \int e_{h_2} \, dt \\ \int e_{l_2} \, dt \\ \vdots \\ \int e_{h_N} \, dt \\ \int e_{l_N} \, dt \end{bmatrix} \tag{7}$$

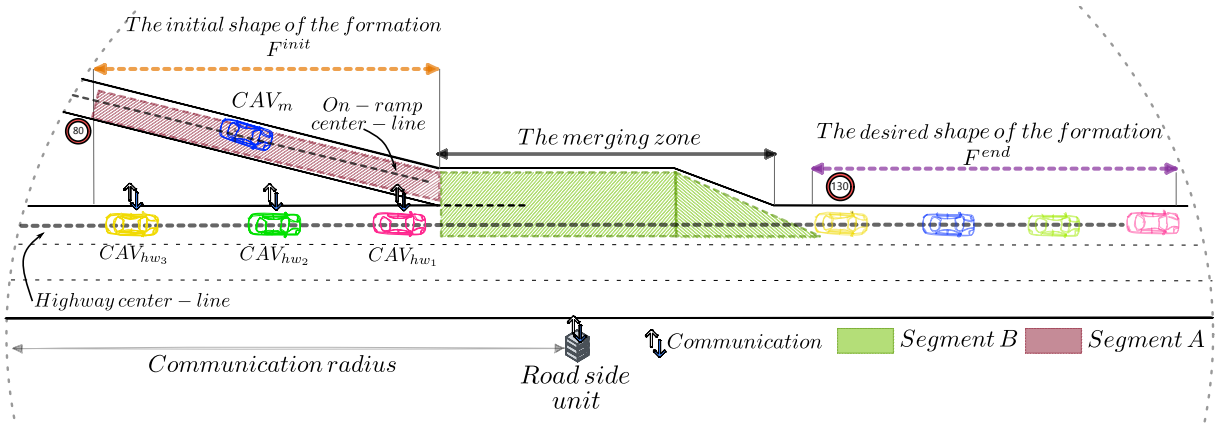

Fig. 2. Illustration of the on-ramp merging on highway scene. The initial shape of the formation of the CAVs under the communication range of the RSU is represented, along with the final desired shape. The *Segment A* representing the zone where the CAV behaves according to the longitudinal motion. In *Segment B* the CAV behaves according to both the longitudinal and the lateral motion.

with Ω_1, Ω_2 and Ω_3 are given in eq. (8).

$$\begin{cases} \Omega_1 = diag[a_{h_1}, a_{l_1}, \cdots, a_{h_N}, a_{l_N}], \\ \Omega_2 = diag[a_{h_1}\lambda_{h_1}, a_{l_1}\lambda_{l_1}, \cdots, a_{h_N}\lambda_{h_N}, a_{l_N}\lambda_{l_N}], \\ \Omega_3 = diag[a_{h_1}\gamma_{h_1}, a_{l_1}\gamma_{l_1}, \cdots, a_{h_N}\gamma_{h_N}, a_{l_N}\gamma_{l_N}], \end{cases} \tag{8}$$

with $\Omega_1^{2N\times 2N}$, $\Omega_2^{2N\times 2N}$ and $\Omega_3^{2N\times 2N}$ are the extended reconfiguration matrices.

Reconfiguration gains: The convergence matrix used in the CORM algorithm [1] assumes that both the longitudinal and the lateral motions converge according to the same convergence rate, which reduces the CORM flexibility. The E-CORM relies on an augmented reconfiguration matrix in eq. (7) to overcome the CORM limitations; namely considering the geometrical limitation encountered with the CORM to fit the reference path of the road (such as the path given by its middle). In fact, separating the longitudinal convergence from the lateral one added more flexibility to the E-CORM. The gains a_{h_i} and a_{l_i} are computed using an optimization procedure that ensures the zero-collision between the CAVs part of the formation. Thus, all the inter-vehicular Euclidean distances must be above a certain safety distance d_{safety}. For further details please confer to [1].

The optimization procedure can be expensive in terms of the computation time. In order to reduce the computation cost, the E-CORM takes advantage from the road topology and the vehicle behavior to optimize only the necessary terms. Figure 3 represents the selection of the coordinates based on the segment in which the CAV_i is located (cf. Figure 2). Thus, when the CAV travels on a segment where only the longitudinal reconfiguration is necessary (cf. Figure 2, Segment A), only the gains related to the longitudinal behavior are optimized, the lateral coordinates l_i are given according to the road center-line. On the other hand, when both of the longitudinal and lateral behaviors are necessary for the reconfiguration (cf. Figure 2, Segment B), both of the gains a_{h_i} and a_{l_i} are optimized. This selection mode is possible thanks to the capacity of the algorithm to guarantee the continuity of the dynamic targets T_d ensured by the formalism using the state S.

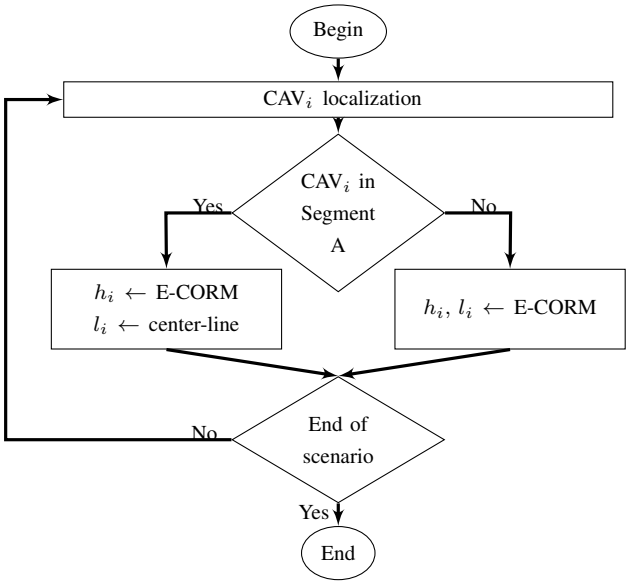

Fig. 3. Coordinates selection based on the traveled segment

Stability analysis w.r.t. the convergence error: The paper is dedicated to the presentation of the AFRS contribution. Thus, the fundamental stability analysis ensured under the E-CORM is given in this section. The stability of the system given in eq. (7) is proved in two steps; 1) the stability analysis of the state S in the system in eq. (4) using a Lyapunov analysis and; 2) the stability of the convergence error e using the system given in eq. (6).

First, it is proposed to define the Lyapunov candidate function:

$$V = \frac{1}{2} S^T S \tag{9}$$

V is a positive-definite function. To guarantee the stability of the system, $\dot{V}$ must be negative-definite. By taking the derivative of eq. (9) and using eq. (5). $\dot{V}$ can be written:

$$\dot{V} = \dot{S}^T S = S^T A^T S \tag{10}$$

Since A^T is a diagonal negative-definite matrix, then $\dot{V} < 0$ and the state S converges asymptotically to zero.

The second step of the stability analysis is to prove the convergence of the formation error system given in (4). The stability analysis of eq. (10) permits to write around the equilibrium point of the state S:

$$\dot{S} = 0 \tag{11}$$

Taking the systems given in eq. (6), eq. (11) and the Laplace transformation, the system can be written as in eq. (12):

$$\begin{aligned} &E_{h_1}p^2 + \lambda_{h_1}E_{h_1}p + \gamma_{h_1}E_{h_1} = 0 \\ &E_{l_1}p^2 + \lambda_{l_1}E_{l_1}p + \gamma_{l_1}E_{l_1} = 0 \\ &\qquad\vdots \\ &E_{h_N}p^2 + \lambda_{h_N}E_{h_N}p + \gamma_{h_N}E_{h_N} = 0 \\ &E_{l_N}p^2 + \lambda_{l_N}E_{l_N}p + \gamma_{l_N}E_{l_N} = 0 \end{aligned} \tag{12}$$

where p is the Laplace operator. The stability of the system given in eq. (12) can be studied as a 2^{nd} order polynomial. According to the Routh-Hurwitz criterion, the system given in (12) is stable if all the terms composing the polynomial have the same sign. Consequently, the sign of the polynomial follows the sign of the formation error e, thus according to Routh-Hurwitz criterion the system given in eq. (6) is stable.

B. Multi-Mode Safe and Efficient Cooperative On-Ramp Merging on Highway

The decision-making level of the AFRS is based on a multi-mode decision-making system. The proposed decision-making algorithm (cf. Figure 4) is in charge of the activation of the appropriate mode based on the risk of collision metric. Two operating modes are integrated in the latter: (a) the nominal mode (cf. Section IV-B1) and (b) the cooperation mode (cf. Section IV-B2). During the activation of the nominal behavior, the safety criterion is continuously tested with the help of the feedback loop, which ensures the respect of the safety criterion. This section is dedicated to draw the explanations about the adopted decision-making system and both of the operating modes.

1) Nominal mode: The goal of the nominal mode is to perform the merging maneuver from the point of view of the merging CAV. This mode takes the assumption of a free merging zone at the merging moment, consequently, no conflicting scenario is considered. The CAV$_m$ is asked to perform the merging scenario while optimizing two sub-criteria objective function: the merging time and its acceleration. The latter is correlated to the energy consumption of CAV$_m$ while performing the merging maneuver.

The nominal mode uses an optimization process to generate the velocity cycle given to CAV$_m$ as an input. The latter is based on the sigmoid function in eq. (13).

$$\mathcal{V}(k) = \mathcal{V}_m^{init} + \frac{\mathcal{V}_m^{desired} - \mathcal{V}_m^{init}}{1 - e^{-\alpha^*(k-\beta^*)}} \tag{13}$$

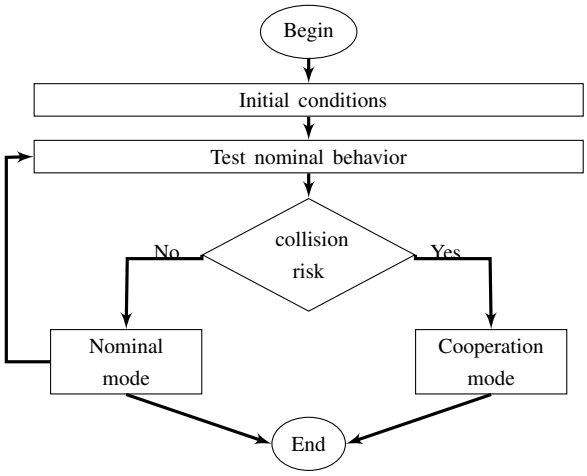

Fig. 4. The proposed multi-mode decision-making system

with $\mathcal{V}_m^{init}$ the initial velocity of CAV_m, and $\mathcal{V}_m^{desired}$ its desired velocity. The latter is based on $\mathcal{V}_{max}$ the maximum authorized velocity by the traffic laws on the traveled segment (cf. Figure 2). α is the convergence rate of the sigmoid function while β is the mid-point time. α^* and β^* are the optimal parameters found by the optimization.

The objective function evaluated to find the optimal sigmoid parameters α^* and β^* is given in eq. (14), it is composed of two sub-criteria weighed with the help of ω_1 and ω_2. 1) The time related cost aims to minimize the required time ($TravelTime$) for CAV$_m$ to perform the merging. 2) The acceleration related cost aims to minimize the variation of the acceleration $a(k)$, $k \in \{1, I_N\}$ during the merging, resulting in an energy efficient merging maneuver from CAV$_m$ perspective.

$$\begin{aligned} \min_{\alpha,\beta} \quad & \omega_1 \frac{TravelTime}{\overline{t}} + \omega_2 \sum_{k=1}^{I_N} \Big(\frac{a(k)}{\overline{a}}\Big)^2 \\ \text{so that} \quad & -4[m/s^2] \leq a(k) \leq 4[m/s^2], \;\; k \in \{1, I_N\} \\ & \mathcal{V}(k) \leq \mathcal{V}_{max}, \qquad\qquad\qquad k \in \{1, I_N\} \end{aligned} \tag{14}$$

$\overline{t}$ and $\overline{a}$ are the normalization terms. They represent respectively, $\overline{t}$ the maximum time needed to perform the maneuver, which is obtained by imposing to CAV_m its initial velocity during the merging, and $\overline{a}$ the maximum acceleration from the acceleration profile $a(k)$.

2) Cooperation mode: The merging zone is a shared topological resource between the CAV$_{hw}$ and the CAV$_m$. The cooperation mode part of the proposed decision-making strategy (cf. Figure 4) is activated when a collision may occur in the merging zone following the nominal behavior (cf. Figure 6). Consequently, the cooperation protocol has the responsibility of setting a conflict-free passing sequence sq of the CAVs in the merging zone. sq will be later translated to a desired virtual shape, which constitutes the input of the E-CORM algorithm in Section IV-A.

Figure 5 presents the flowchart of the cooperation mode. The first step consists of replaying the nominal scenario in

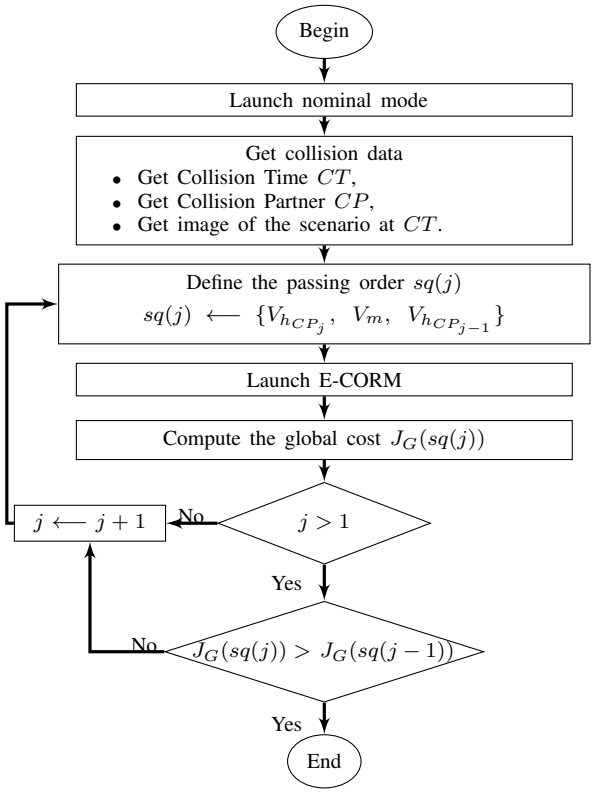

Fig. 5. Flowchart representing the step sequence of the cooperation mode

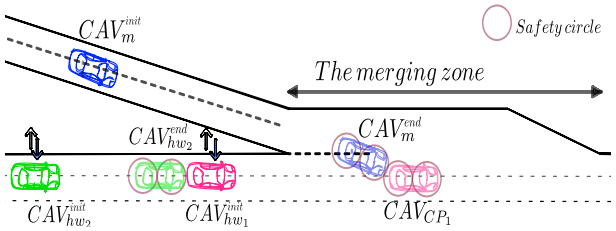

Fig. 6. Image of the merging scenario at $t = CT$

order to predict the state of the merging scene at the Collision Time CT (cf. Figure 6). The predicted data are listed in the second step of the flowchart (cf. Figure 5). Figure 6 gives a visual explanation of the latter, where a screen-shot of the merging scenario was taken at CT. The id-list of the CAVs under the communication range of the RSU at CT is created. The latter will be used by the passing sequence procedure sq. Each passing order will be evaluated with the help of the global objective function presented below.

The Global objective function: the global cooperation function J_G is used to evaluate the level of cooperation related to the different passing sequences sq. It uses the initial conditions of the CAV$_{hw}$ as a reference to define the coordination effort and the nominal mode to compare the performance of the CAV$_m$, it can be written as:

$$J_G(sq(j)) = \sum_{i=1}^{N} \omega_i J_i \tag{15}$$

where

$$\sum_{i=1}^{N} \omega_i = 1 \tag{16}$$

ω_i represents the participation weight given to the CAV$_i$ and it respects the expression given in eq. (16). $i \in \mathcal{N}$ represents the index of the N CAVs part of the considered formation. J_i given in eq. (17) is the individual cost related to each considered CAV.

$$J_{\substack{i \\ \forall i \in \mathcal{N}}} = \omega_{safe} J_i^{Safe} + \omega_{Acc} J_i^{Acc} + \omega_{KE} J^{KE} + \omega_n J^{NC} \tag{17}$$

with:

$$\omega_{safe} + \omega_{Acc} + \omega_{KE} = 1 \tag{18}$$

$$\omega = \{\omega_{safe}, \omega_{Acceleration}, \omega_{KE}, \omega_{NC}\} \tag{19}$$

ω is the set containing the participation weights given to each sub-cost part of the individual cost J_i. The cost J_i is composed of the four components described above:

(a) The safety related cost J_i^{Safe} considers the Euclidean inter-vehicular distances in between the CAVs part of the formation. It can be written as in eq. (20):

$$J_i^{Safety} = \frac{\sum_{k=1}^{I_S} \frac{1}{EucDist\{X_{V_i}(k), X_{V_j}(k)\}_{\forall i \in \mathcal{N}}^{\forall j \in \mathcal{N}, j \neq i}}}{\sum_{k=1}^{I_S} \frac{1}{d_{Safety}}} \tag{20}$$

d_{safety} is the safety distance that needs to be always respected between the CAVs. It corresponds to twice the radius of the safety circle around the CAV (cf. Figure 6). It is used here to normalize the safety cost.

(b) The cost related to the dynamics of the CAVs J_m^{Acc} utilizes the acceleration. The latter aims to minimize the gap between the nominal dynamic and the cooperation-based dynamic related to CAV_m, $\forall m \in \mathcal{M}$.

$$J_{\substack{m \\ \forall m \in \mathcal{M}}}^{Acc} = \Big| \frac{1}{I_{Nominal}} \sum_{k=1}^{I_{Nominal}} \Big[\frac{a_m^{nominal}(k)}{\overline{a_m^{nominal}}}\Big]^2 - \frac{1}{I_S} \sum_{k=1}^{I_S} \Big[\frac{a_m^S(k)}{\overline{a_m^S}}\Big]^2 \Big| \tag{21}$$

As for the highway-CAVs their dynamic is minimized with the cost $J_{\substack{hw \\ \forall hw \in \mathcal{H}}}^{Acc}$.

$$J_{\substack{hw \\ \forall hw \in \mathcal{H}}}^{Acc} = \frac{1}{I_S} \sum_{k=1}^{I_S} \Big[\frac{a_{hw}^S(k)}{\overline{a_{hw}^S}}\Big]^2 \tag{22}$$

with a_m^S and a_{hw}^S being respectively, the acceleration profile of the CAV_m and CAV_{hw} during the merging scenario under the cooperation mode. $\overline{a_m^{nominal}}$ and $\overline{a_m^S}$ are the maximum acceleration with the nominal mode (cf. Section IV-B1) and with the cooperation mode, respectively. The latter are used to normalize the acceleration cost.

(c) The cost related to the energy cost generated by the cooperation is characterized by the kinetic energy used by the CAVs. The kinetic energy related cost has two objectives: 1) it gives the energy consumption of the CAV

even at a constant acceleration. 2) Since it includes the weight of the CAV, it allows a distinction of the efforts asked to be done by a truck and a light-weight CAV.
Same as for the dynamic related cost, the nominal dynamic (cf. Section IV-B1) is used to evaluate and minimize the gap between the nominal mode dynamic and the cooperation one. Thus, the kinetic energy cost for the merging CAV is shown in eq. (23).

$$J^{KE}_{\substack{m \\ \forall m \in \mathcal{M}}} = \frac{1}{2} m_{V_m} \Big| \frac{1}{I_{Nominal}} \sum_{k=1}^{I_{Nominal}} \Big[\frac{\mathcal{V}_m^{nominal}(k)}{\overline{\mathcal{V}_m^{nominal}}} \Big]^2 - \frac{1}{I_S} \sum_{k=1}^{I_S} \Big[\frac{\mathcal{V}_m^S(k)}{\overline{\mathcal{V}_m^S}} \Big]^2 \Big| \tag{23}$$

The kinetic energy related to the highway CAVs is noted J^{KE}_{hw} (cf. eq. (24)).

$$J^{KE}_{\substack{hw \\ \forall hw \in \mathcal{H}}} = \frac{1}{2} m_{V_{hw}} \Big(\frac{1}{I_S} \sum_{k=1}^{I_S} \Big[\frac{\mathcal{V}^S_{ref}(k) - \mathcal{V}^S_{hw}(k)}{max(\mathcal{V}^S_{ref}, \mathcal{V}^S_{hw})} \Big]^2 \Big) \tag{24}$$

with m_{V_i} being the weight of the CAV_i. $\mathcal{V}^S_m$ and $\mathcal{V}^S_{hw}$ are the velocity profiles of both CAV_m and CAV_{hw} during the merging scenario under the cooperation mode respectively. $\mathcal{V}^S_{ref}$ is the desired velocity of the CAV_{hw}. The term $max(\mathcal{V}^S_{ref}, \mathcal{V}^S_{hw})$ is used for the normalization of the kinetic energy cost.

Altruistic passing sequence: The fourth term of the individual cost function is the non-collaborative cost, its objective is to ensure the avoidance of extensive cooperation efforts from the perspective of the CAV$_{hw}$. In fact, the highway CAVs are said to be altruistic, in other terms, they are set as collaborative by definition. However, the Boolean cost plays the role of the cooperation threshold from the CAV_{hw} perspective. The threshold is computed based on the percentage of the cooperation of the considered CAV_{hw_i}. Consequently, when a passing order sq orders the CAV_{hw_i} an effort above its effort's threshold, the non-collaborative cost is maximized.

V. Simulation Results

In order to evaluate the efficiency of the proposed AFRS in terms of its ability to guarantee a safe and smooth CAV dynamics while performing the on-ramp merging on highway, it is proposed to discuss the results of both the nominal mode and cooperation mode.

1) On-ramp merging operated by the nominal mode: In the following simulation, it is aimed to perform the merging scenario according to the nominal mode. The CAV$_m$ initial pose is set to respect the non-collision metric in order to activate the nominal mode, in addition to a proper spacing of the CAV$_{hw}$ w.r.t. CAV$_m$. The simulation video can be found in: shorturl.at/HMVZ9

The Figure 7 presents the Euclidean in-between distances. During the merging scenario it can be noticed that both the

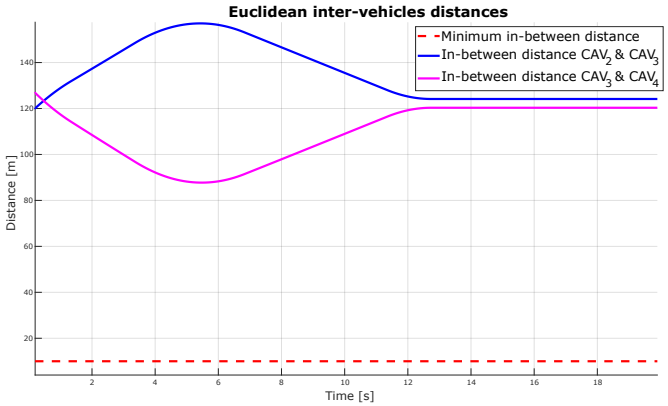

Fig. 7. Nominal mode: the distances between the CAVs.

distance between the CAV$_m$ (CAV$_3$) and the CAV$_{2,4}$ are above d_{safety} meaning that the safety requirement is ensured while the nominal mode is running the merging scenario. As for the velocity cycles generated by the control law in the Figure 8, the maximum authorized velocity (80 km/h in segment A and 130 km/h in segment B) is respected by all the CAVs.

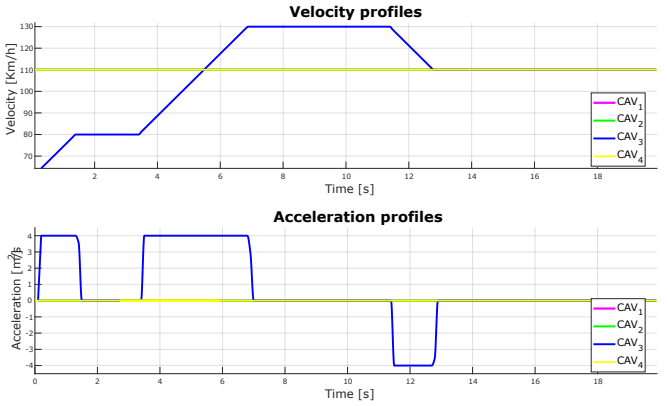

Fig. 8. Nominal mode: the dynamics of the CAVs.

2) On-ramp merging operated by the cooperation mode: In the following simulation, it is aimed to perform the merging scenario according to the cooperation mode. The CAV$_m$ initial pose is set to activate the non-collision metric when the merging is operated by the nominal mode, the simulation video can be found in: shorturl.at/gjGKL

TABLE I
Numerical results of the cooperation mode

sq	V$_1$,V$_2$,V$_4$,V$_3$				V$_1$,V$_2$,V$_3$,V$_4$			
J$_G$	**0.1159**				0.1642			
CAV	V1	V2	V3	V4	V1	V2	V3	V4
J$_{safety}$	0.0705	0.0884	0.1058	0.1031	0.0871	0.0894	0.1451	0.1031
J$_{acceleration}$	0	0	0.1290	0.0571	0	0	0.1188	0.0971
J$_{Energy}$	0	0	0.0574	0.1159	0	0	0.1405	0.1509

The passing sequence selected by the cooperation mode is $sq = \{CAV_1, CAV_2, CAV_4, CAV_3\}$ (cf. Table I). The Euclidean distance between the CAVs are given in Figure 9, where conflict between the CAV$_m$ (CAV$_3$) and the CAV$_4$ has

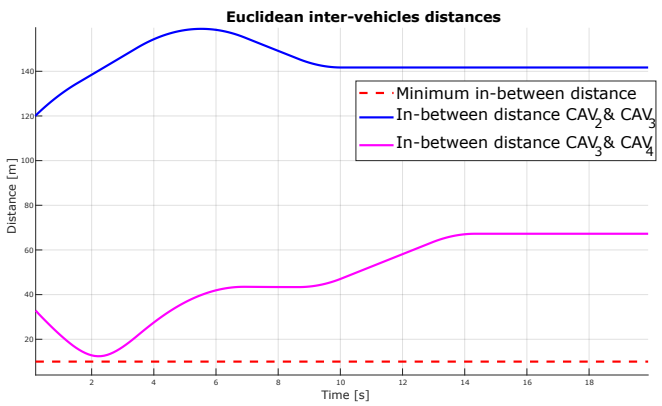

Fig. 9. Cooperation mode: the distances between the CAVs.

been solved, in addition to guaranteeing that all the in-between distances are above d_{safety}. The velocity profile of the CAV_4 corresponds to the selected passing sequence sq (cf. Table I). The velocity profiles respect the maximum authorized velocity (80 km/h in segment A and 130 km/h in segment B). The acceleration profile respects the maximum and minimum authorized limits.

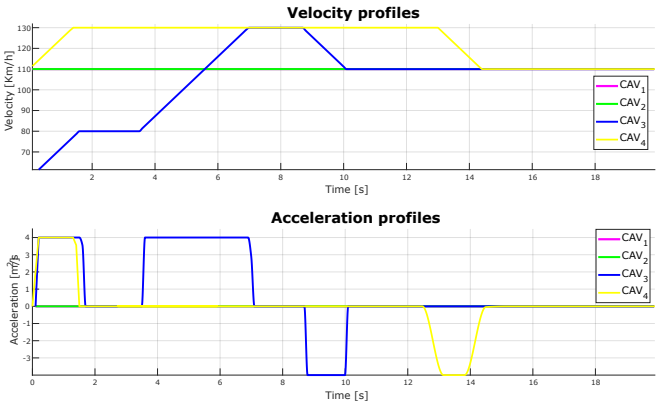

Fig. 10. Cooperation mode: the dynamics of the CAVs.

VI. Conclusion and Perspectives

This paper proposed an Altruistic Formation Reconfiguration Strategy (AFRS) for on-ramp merging on highway based on two levels: 1) the multi-mode decision-making level, responsible of the activation of the appropriate behavior based on the safety metric. Two behaviors are proposed under the decision-making level: (a) the nominal behavior, designed to perform the merging from the merging CAV perspective, (b) the cooperative mode, activated by the decision-making level when the safety requirement is not satisfied by the nominal mode. Its objective is to generate the optimal passing sequence from the formation perspective. 2) The proposed planning level, composed of two planners attached to both modes in the decision-making level: (a) The optimal velocity cycle generator under the nominal mode has the responsibility to minimize the time spent in the merging zone, in addition, to the energy consumption of the merging CAV. (b) The proposed Extended Constrained Reconfiguration Matrix (E-CORM) that takes into account the passing sequence generated by the cooperation mode to perform a safe and feasible coordination of the formation motion during the merging phase. The future works based on the AFRS algorithm will mainly consider the implementation on real vehicles available in the laboratory.

Acknowledgment

This work received the support of the French government and the CPER RITMEA, Hauts-de-France region.

References

[1] L. Saidi, L. Adouane and R. Talj, CORM: Constrained Optimal Reconfiguration Matrix for Safe On-Ramp Cooperative Merging of Automated Vehicles, in IEEE ITSC, pp. 2783-2790, Macao, China, Sept-Oct 2022.

[2] A. Vahidi and A. Zambonelli, Coordination infrastructures for future smart social mobility services, in IEEE Intelligent Systems, vol. 29, pp. 78–82, 2014.

[3] J. Rios-Torres and A. A. Malikopoulos, A survey on the coordination of connected and automated vehicles at intersections and merging at highway on-ramps, in IEEE Trans. on Intelli. Transp. Sys., vol. 18, pp. 1066-1077, 2017.

[4] A. Sassi and F. Sciaretta, Energy saving potentials of connected and automated vehicles, in Transportation Research Part C: Emerging Technologies, vol. 95, pp. 822–843, 2018.

[5] J. Vilca, L. Adouane and Y. Mezouar, Stable and Flexible Multi-Vehicle Navigation Based on Dynamic Inter-Target Distance Matrix, IEEE Trans. on Intelli. Transp. Sys., vol 20, pp. 1416-1431, 2019

[6] K. Drasner and P. Stone, A Multiagent Approach to Autonomous Intersection Management, in Journal of Artificial Intelligence Research, vol. 31, pp. 591-656, 2008.

[7] L. Chen and C. Englund, Cooperative Intersection Management: A Survey, in IEEE Trans. on Intelli. Transp. Sys., vol. 17, pp. 570-586, 2016.

[8] H. Liu, W. Zhuang, G. Yin, Z. Li and D. Cao, "Safety-Critical and Flexible Cooperative On-Ramp Merging Control of Connected and Automated Vehicles in Mixed Traffic," in IEEE Trans. on Intelli. Transp. Sys., vol. 24, no. 3, pp. 2920-2934, 2023.

[9] T. Chen, M. Wang, S. Gong, Y. Zhou and B. Ran, Connected and automated vehicle distributed control for on-ramp merging scenario: a virtual rotation approach, in Transportation Research Part C: Emerging Technologies, Vol. 133, pp. 103451, 2021.

[10] A. Uno, T. Sakaguchi, and S. Tsugawa, A merging control algorithm based on inter-vehicle communication, in Proc. IEEE/IEEJ/JSAI Int. Conf. Intell. Transp. Syst., pp. 783–787, Tokyo, Japan, Oct 1999.

[11] Z. Wang, G. Wu, and M. Barth, Distributed consensus-based cooperative highway on-ramp merging using v2x communications, in SAE Technical Paper, 2018.

[12] S. D. Kumaravel, A. A. Malikopoulos and R. Ayyagari, "Decentralized Cooperative Merging of Platoons of Connected and Automated Vehicles at Highway On-Ramps," 2021 American Control Conference (ACC), pp. 2055-2060, New Orleans, LA, USA, 2021.

[13] H. Xu, S. Feng, and Y. Zhang, A Grouping Based Cooperative Driving Strategy for CAVs Merging Problems, in IEEE Trans. on Intelli. Transp. Sys., pp. 6125-6136, 2019.

[14] F. Zhu, S. Easa, and K. Gao, Merging control strategies of connected and autonomous vehicles at freeway on-ramps: a comprehensive review, in IEEE Journal of Intelli. and Connec. Veh., pp. 99-111, 2022.

[15] L. Xu, J. Lu, B. Ran, F. Yang, J. Zhang, Cooperative merging strategy for connected vehicles at highway on-ramps. Journal of Transp. Eng., Part A: Systems, vol. 145, no 6, pp. 04019022, 2019.

[16] A. De luca, G. Samson and C. Samson, Feedback control of a non-holonomic car-like robot, in Robot Motion Planning and Control, ed J.P. Laumond, vol 229, pp. 171-253, 1998.

[17] J. Vilca, L. Adouane, Y. Mezouar, and P. Lebraly, "An overall control strategy based on target reaching for the navigation of an urban electric vehicle," in Proc. IEEE/RSJ Int. Conf. Intell. Robots Syst., pp. 728–734, 2013.